Molecular Crystals and Liquid Crystals Science and Technology. Section A. Molecular Crystals and Liquid Crystals
Publication details, including instructions for authors and subscription information:
http://www.tandfonline.com/loi/gmcl19

Surface Reconstruction and Finite-Size Effects in Smectic Free Standing Films

Ewgeni Demikhov [a]

[a] Institute of Physical Chemistry, University of Paderborn, 33095, Paderborn, Germany

Version of record first published: 04 Oct 2006.

To cite this article: Ewgeni Demikhov (1995): Surface Reconstruction and Finite-Size Effects in Smectic Free Standing Films, Molecular Crystals and Liquid Crystals Science and Technology. Section A. Molecular Crystals and Liquid Crystals, 265:1, 403-434

To link to this article: http://dx.doi.org/10.1080/10587259508041710

Mol. Cryst. Liq. Cryst. 1995, Vol. 265, pp. 403–434
Reprints available directly from the publisher
Photocopying permitted by license only

SURFACE RECONSTRUCTION AND FINITE-SIZE EFFECTS IN SMECTIC FREE STANDING FILMS

EWGENI DEMIKHOV
Institute of Physical Chemistry, University of Paderborn, 33095 Paderborn, Germany

Abstract Surface ordering phenomena and finite-size effects determine properties of free standing films by decreasing the number of layers. Computer simulations have shown that the boundary layers reconstruction can cause a disappearence of the first order Sm A - Sm C* phase transition by deminishing the number of layers. Whithin the wetting analogy it is shown that the surface tension temperature dependence correlates with the type of surface ordering in free standing films. Finite-size effects of two categories are discussed: i) dependence of thermodynamic parameters on the system size (finite-size scaling), ii) destruction of the long-range order by thermal fluctuations in a sence of Landau-Paierls theorem and related effects (dimensional crossover). Anomalous experimental properties of the free suspended films with high spontaneous polarization are studied. The dimensional crossover is investigated for nonferroelectric and ferroelectric smectic phases with high spontaneous polarization.

1 Introduction. Anisotropic liquid systems with confined dimension.

Influence of dimension on phase transitions in physical systems is established for a long time [1]-[3]. There exists considerable theoretical literature about dimension effects in thermodynamics, but the situation with experiment is less satisfactory. The problem is to find an appropriate system, where predictions of theory can be tested with a good precision.

Anisotropic liquids have many advantages for experimentators: the great number of different molecular structures and order parameters essencially increase spectrum of problems, which can be formulated and solved. In polymer dispersed liquid crystals (PLDC) used in electrically adressable displays [4] a low molecular weight liquid crystal is surrounded by an anisotropic or isotropic polymer matrix. Stable configurations of the director field in liquid crystalline droplets are determined by a competition between the elastic energy of a liquid-crystalline phase and the surface energy on a polymer -liquid crystal boundary. In samples with a large surface to volume ratio the thermodynamically stable bulk configuration of a liquid crystalline phase can be completely changed by surface effects.

Discotic liquid crystals can form self-confined free suspended threads [5, 6]. To form a strand a small amount of a compound should be placed between two pivots, the sample heated to the temperature interval of a discotic phase and the pivots are drown apart. One can produce mechanically stable threads several micrometers in diameter and several hundreds micrometers in length. Interesting dimensional effect

is found in [5]: in very thin threads (about 1 μm in diameter) the discotic director is tilted with respect to the column axis in D1 phase and rotates around it in the nonchiral triphenylene- n-dodecanoate.

Two-dimensional films of organic molecules on the interface oil-water [7] is an example of plane liquid systems confined by a liquid surrounding.

Free-standing films of smectic liquid crystals are self-confined plane systems with number of layers ranging in the interval (2 - 1000) [8] - [14]. They are stable against rupture, because of the 'rigidity' of smectic layers. Thickness of the films is homogeneous and can be exactly measured by spectroscopic methods.

General difficulty by investigation of confined systems is the influence of the boundary. Self-confined systems are with no doubt preferencial for study of dimension effects, because properties of liquid crystals confined by a liquid or solid surrounding substantially depend on their material constants and structure.

2 General description of order in free standing films

2.1 Positional and orientational order

It is well known that the mean square fluctuation of molecules position in crystalline phases does not depend on the sample size and can be expressed as:

$$\sqrt{< u^2 >} \sim k_b T \tag{1}$$

If the density functional ρ depends on one coordinate, the average layer displacement amplitude diverges at large distances logarithmically [15, 16] :

$$\langle u^2(r) \rangle \approx \frac{k_b T}{4\pi\sqrt{KB}} ln \frac{\sqrt{LK/B}}{a_0}, \tag{2}$$

where L is the film thickness; a_0 is a molecular diameter; B is the elastic constant assosiated with compression of smectic phase; K is the elastic constant describing the long wave layer undulations. This result forbids existence of phases with one dimensional density modulation. Using typical values for parameters in eqn.(2): $K \sim 10^{-6}$ dyn, $B \sim 2.5 \times 10^7$ dyn/cm^2, $a_0 \sim 4\mathring{A}$, one can estimate that the sample size where the mean fluctuation of the smectic layers position is of the order of the interlayer spacing ($\sim 30\mathring{A}$) is equal to e^{270} cm. Normally one works with the 0.06-10 μm free standing films. For a 1μm film and T=300 K one obtains:

$$\sqrt{\langle u^2(r) \rangle} \approx 5\mathring{A} \tag{3}$$

Therefore, smectic phases are relatively stable in thin films.

Three types of the in-plane order in smectic phases can be considered: a chiral in-plane order [17, 18, 19], an achiral in-plane order [53] and the hexatic order. It is convenient to describe two-dimensional structures in free standing films with a vector

order parameter **c**, which points in the direction of the tilt and its amplitude is equal to the projection of the director onto the smectic plane. P. Gennes has predicted [17] a possibility of a chiral in-plane configuration of the **c** vector field with an axis parallel to the smectic planes. This result is due to the lack of symmetry center in chiral smectic phases and a necessity to take into account the term linear in $(\mathbf{n}\cdot curl\mathbf{n})$ in the elastic free energy. This idea was elaborated by Langer and Sethna [18] and Hinshaw et al. [19]. In accordance with results of these works two dimensional director **c** can built-up a one dimensionally periodical system of discontineous walls [18, 19] (striped state) or two dimensional array of intersecting +1 walls and -1/2 disclinations with a hexagonal symmetry (hexagonal state) [19]. The case of thin smectic films was considered, but the predictions should be relevant to the bulky samples [19]. Structures of this type has not been experimentally observed until now.

The concept of the hexatic ordering was introduced in [20] - [22]. In accordance with Halperin-Nelson melting theory the transformation solid-liquid proceeds in two steps: the first stage is the unbinding of dislocations, which destroys positional order and the second stage is the unbinding of disclinations, which destroys orientational order. Positional correlations in a two -dimensional crystal are described by a function $G_\rho(\mathbf{r})$:

$$G_\rho(\mathbf{r}) = \langle\rho(\mathbf{r})\rho(0)\rangle - \rho_0^2, \tag{4}$$

where ρ_0 is the average density of the system. The orientational order in hexatic phases is described as:

$$\Psi_6 = \langle\exp i6\theta(\mathbf{r})\rangle, \tag{5}$$

where θ is an angle between the bond orientation and some coordinate axis. Appropriate correlation function is

$$G_6(\mathbf{r}) = \langle\Psi_6(0)\Psi_6^*(\mathbf{r})\rangle \tag{6}$$

Smectic C phase possesses no hexatic order and orientational correlations are described by the correlator of the vector **c** projections:

$$G_c = < c_\alpha(0)c_\beta(r) > \sim \delta_{\alpha\beta}r^{-\Delta(T)}, \tag{7}$$

where c_α are components of the two-dimensional vector order parameter. Crystalline and smectic phases are characterized by the following asimptotic behaviour of correlation functions for the in-plane order:

3D-Crystalline order	$\lim_{r\to\infty} G_6(r) = const \neq 0,$
	$\lim_{r\to\infty} G_\rho(r) = const \neq 0$
Hexatic order	
(Sm B, F, I)	$\lim_{r\to\infty} G_6(r) \sim r^{-\eta};$
	$\lim_{r\to\infty} G_\rho(r) \sim \exp(r/\xi)$
smecic C phase	$\lim_{r\to\infty} G_c(r) \sim r^{-\Delta(T)};$
	$\lim_{r\to\infty} G_\rho(r) \sim \exp(r/\xi)$
smectic A phase	$\lim_{r\to\infty} G_6(r) \sim \exp(-r/\xi);$
	$\lim_{r\to\infty} G_\rho(r) \sim \exp(-r/\xi)$

In the isotropic liquid both positional and orientational order decay exponentially. The concept of hexatic order was very productive and after brilliant series of

experimental and theoretical work of several groups (see [12], [23] -[31]) the phase sequence, predicted in two-dimensional melting theory has been verified.

2.2 Suppression of thermal fluctuations in two-dimensional systems by surface tension and dipolar interaction

In [16] was shown that in thin free standing smectic films the average layer position fluctuation is essentially suppressed near the surface by effects of surface tension. For example, on the boundary of a 35-layer film $\sqrt{\langle u^2(r)\rangle} \approx$ 1-2 $\AA$, whereas in the middle 4-5 $\AA$ for the surface tension coefficient $\alpha \approx$100 dyn/cm.

Fluctuations of the vector **c** in ferroelectric films are combined with the appearence of the polarization charge with a density $\rho \sim$-div$\mathbf{P}$, where $\vec{P}$ is the local polarization vector perpendicular to the molecular tilt plane. The Coulomb interaction:

$$F_P = \frac{1}{2}\int \frac{d^2r d^2r'}{\mid \vec{r} - \vec{r'} \mid} \frac{\partial}{\partial r_\alpha} \frac{\partial}{\partial r'_\beta} P_\alpha(\vec{r}) P_\beta(\vec{r'}), \tag{8}$$

prevents development of thermal fluctuations and a long range orientational order becomes possible. In [32] - [34] a possibility of a new phase transition between a high temperature isotropic phase and a low temperature anisotropic ferroelectric phase was shown. In contrast to (7) the mean square fluctuation of the vector **c** in the anisotropic state becomes a finite value [34].

The phase transition into the anisotropic state should be expected in films with high spontaneous polarization. A criteria for such a phase transition was formulated in [33]. Let us consider a dependence of an average order parameter on the system size L. The order parameter can be written in the form:

$$\psi = \frac{|< \vec{P} >|}{P}. \tag{9}$$

The typical length L_g, which characterizes the suppression of the thermal fluctuations by the dipolar interaction, can be estimated as:

$$L_g \sim \frac{K}{2\pi P^2}, \tag{10}$$

where K is an elastic constant. For the distances $L \leq L_g$ there is no preferencial orientation of c-director and orientational order is destroyed by thermal fluctuations. The order parameter ψ scales as $(L/a)^{-\eta_1}$, where a is film thickness and η_1 is a positive exponent. For $L \geq L_g$ $\psi \sim const.$ We shall call this state of ferroelectric films a weak anisotropic state in an analogy with ferromagnets [35].

Because the free standing films are combined of more than one layers, they are strictly speaking not two-dimensional. Therefore, some bulky structures can be competitive with the weak anisotropic state.

2.3 Critical behaviour in confined systems

As already mentioned, there is a great number of theoretical investigations about finite-size scaling in systems undergoing second order phase transitions (see [2, 3] and references therein). Two simplest effects can be expected: shifting of the phase transition temperature and rounding of pretransitional characteristics.

The dependence of the second order transition temperature on the system size L is described by the following expression:

$$(T(L) - T(\infty)) \sim L^{-\lambda}, \tag{11}$$

where T(L) is a phase transition temperature in a confined system; T(∞) is a transition temperature of the bulky sample; λ is a shifting exponent.
The rounding of the pretransitional characteristics is described by a scaling function for a temperature interval, over which the phase transition is smeared:

$$\Delta T \sim L^{-\lambda}, \tag{12}$$

In several experiments it was found that the boundary layers in free standing films are reconstructed with respect to the inner layers. Several situations are possible (figure 1):

1. the structure in the boundary layers is different with respect to the inner layers and corresponds to some low temperature phase of the material [36] (figure 1a);

2. the boundary layers possess a different symmetry with respect to the inner layers but their structure is stable only in ultrathin films and is not observed in the bulk [36].

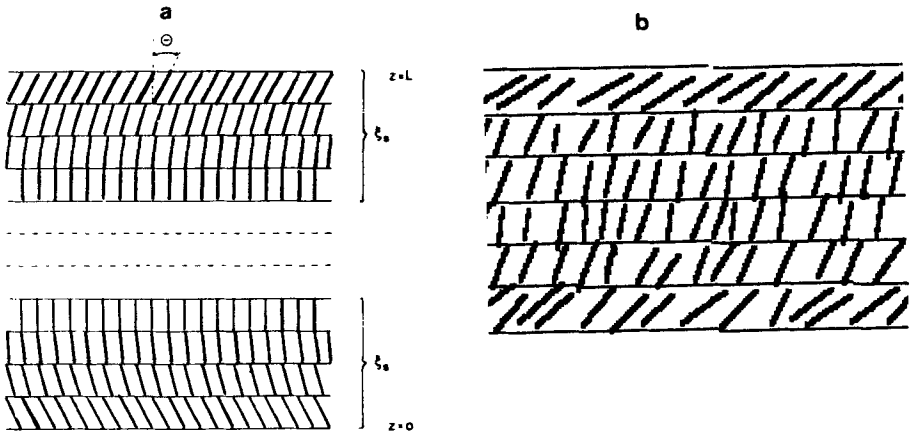

Figure 1. Relation between the structures in the boundary and inner layers: (a) symmetry of boundary and inner layers are different; (b) boundary and inner layer possess the same symmetry but different order parameters.

3. the boundary layers possess the same symmetry as inner layers, but a different order parameter [37] (figure 1b).

The penetration length of the surface order ξ_s is a function of temperature, which depends on the type of the intermolecular interaction (long- or short- range), the roughness of the boundary between the surface ordered phase and the interior of the film [38] - [41]. If the intermolecular interactions are the long-range order van der Waals forces, the penetration length of the surface ordered or disordered phase obeys to the law

$$\xi_s \sim t^{-1/3}, \tag{13}$$

where t=| $T - T_c$ | $/T_c$, T_c is a transition temperature. In the case of short -range interactions a logarithmic temperature dependence of the surface reconstructed layer is expected to be:

$$\xi_s \sim ln(1/t) \tag{14}$$

The surface layer in solids is less ordered than the bulk, because the number of chemical bonds for a molecule on the surface is smaller. The boundary layers in free standing films possess usually a higher order parameter with respect to the inner layers because of the influence of the surface tension. The above mentioned temperature dependences of the penetration length were experimentally proved recently by calorimetry measurements [43] and computer enchanced optical microscopy [42].

When the penetration length of the surface order is comparable with the film thickness, one can expect a shift of the transition to higher temperatures (case 1,2). In the case 2 a new phase appears on the phase diagram in the ultrathin films. Thus, there are two qualitatively different physical reasons for the transition temperature shift: surface ordering and finite-size scaling. To distinguish contributions of both effects in experiment is difficult, because usually some integral characteristics are measured.

Dimensional crossover means a change of a system behaviour from three dimensional to two dimensional laws. According to the Landau -Paierls theorem the decrease of size results generally in a decrease of the order parameter of the system. This effect can be suppressed by the influence of the surface tension or by effects of the long-range dipolar interaction. The first experimental study of high spontaneous polarization effects on stable director field configurations in free standing films is reported in this paper.

3 Experimental properties of smectic membranes.

The first step in investigation of free standing films is to draw a film and to control the number of layers. In early works [8] free standing films were produced by wiping a small amount of material in a smectic phase over a hole in a glass slide. Such films are stable during a valuable time interval, whereas nematic and cholesteric free standing films are unstable. A more convenient method for the film drowing has been used in [13].

In the current work we have produced free standing films on a rectangular frame with one mobile side. The frame was mounted in a closed thermostabilised metalic support in a focal plane of a Leitz Orthoplan microsope. The temperature of films was regulated with an accuracy $\pm$ 0.01 °C. Using this frame we were able to produce films with a controled number of layers. In microscopic texture studies one can detect image changes in films with 2 - 1000 layers.

In ultrathin films (N = 2-15 layers) the number of layers is usually determined with a high precision by the laser reflectivity measurements. In [13, 44] and in the present work the films reflectivity has been measured in the whole interval of visible wavelength, which after a fitting procedure gives the exact number of layers for N~2-300. The scheme of experimental set-up is shown on figure 2. Optical thickness of the film and the refractive index are parameters, which can be determined from the reflectivity measurements. To find them the reflectivity curves were fitted with classical optics expressions for the multiple beam interference in a plan parallel plate [45]:

$$I(\lambda) = \frac{f sin^2(\frac{2\pi D}{\lambda})}{1 + f sin^2(\frac{2\pi D}{\lambda})}, \tag{15}$$

where

$$f = \frac{(n^2 - 1)}{4n^2}, \tag{16}$$

D=N n d is the optical thickness of the whole film, N is the number of layers, n is the refractive index and d is the average interlayer spacing.

To apply these expressions correctly one has to proceed with very narrow light beams, because of the non-zero curvature of films. Sensitivity of this method is enough to resolve spectral changes after removing one smectic layer.

In [8]-[9], [46] the elastic coefficient, polarization and viscosities of free standing films have been investigated by means of light scattering. Director field configurations and defects were studied in [11], [18, 19], [47] - [53]. Hexatic ordering in free standing films has been investigated in [23]- [31]. The surface ordering problem has been

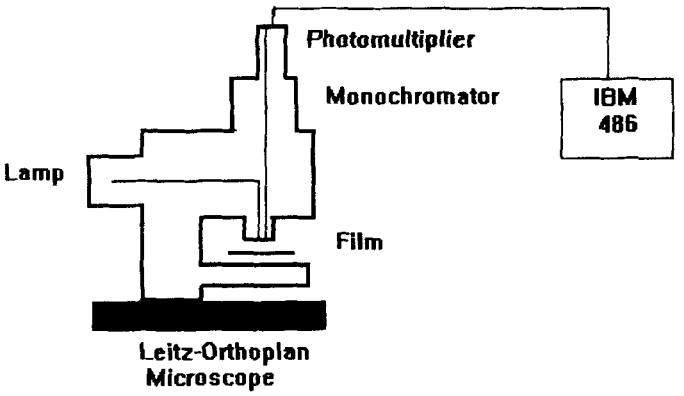

Figure 2. Experimental set-up for film reflectivity measurements and visual observations.

discussed in [54] - [56], electric field effects in [57], dimensional effects on the phase transitions in [36, 44, 58].

4 Surface reconstruction in free standing films

4.1 Surface stabilized phases in liquid crystals

One of the pronounced dimension effects on the phase transitions in free standing smectic films is the dependence of the phase diagram on the number of layers observed by Pershan et al. [36]. New smectic phases appear on the 7O.7 phase diagram: smectic F phase for $N \leq 180$ and smectic I phase in films thinner than 25 layers.

Figure 3 shows the phase diagram of achiral 4-n- penthyloxybenzylidene -4-n- hexylaniline (5O.6) studied by the optical microscopy. Bulky samples of this material possess following liquid-crystalline phases (transition temperatures are given in degrees centigrade): cryst (34.5) smectic G (40.3) smectic F (43) cryst B (51) smectic C (53) smectic A (61) nematic (73) isotropic.
A schlieren texture is intrinsic for the smectic A phase due to the tilted Sm C boundary layers. The contrast of the schlieren texture depends on the tilt angle of the director on the boundary.

In films thiner than 33 layers a new texture with a two-dimensional periodicity appears on the phase diagram in the temperature interval of the smectic C phase (figure 4). Such kind of textures has been observed in [52], where it was argued to be the smectic L phase. A general discussion of possible director field structures relevant to this case was given in [53]. An intersting observation was made during the phase transition smectic F- smectic B on heating (figure 5). The density of the smectic B phase is larger than of smectic F and the diffusion of material between the two phases is very slow. During the phase transition on heating the film breaks

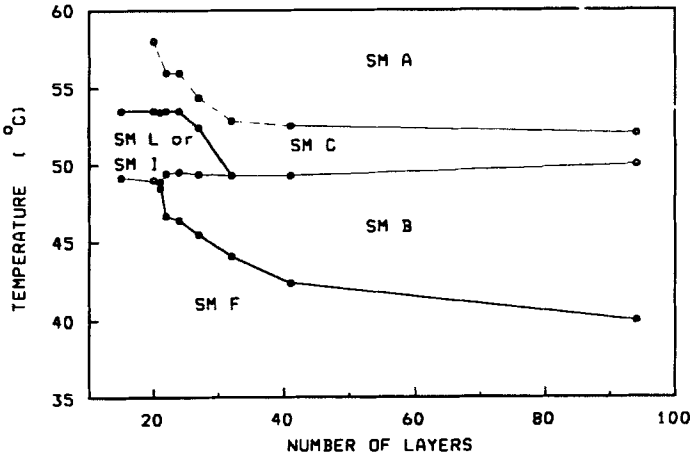

Figure 3.Phase diagram of 5O.6.

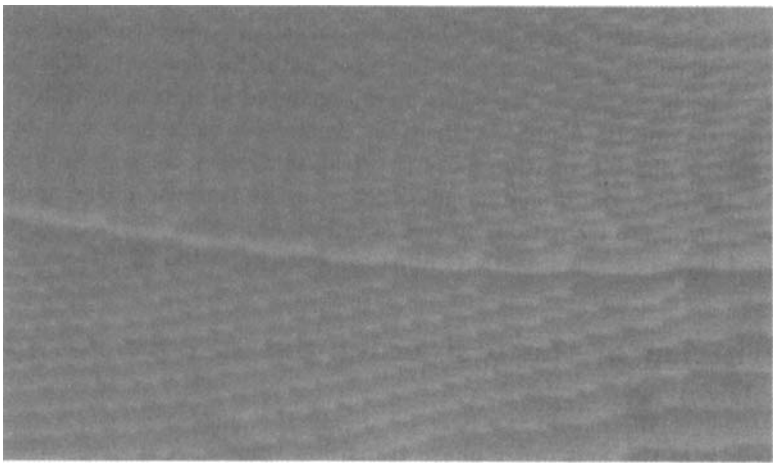

Figure 4. Image of a smectic phase (Sm I or Sm L) occuring on the 5O.6 phase diagram in ultrathin films ($N \leq 33$). See Color Plate XIV.

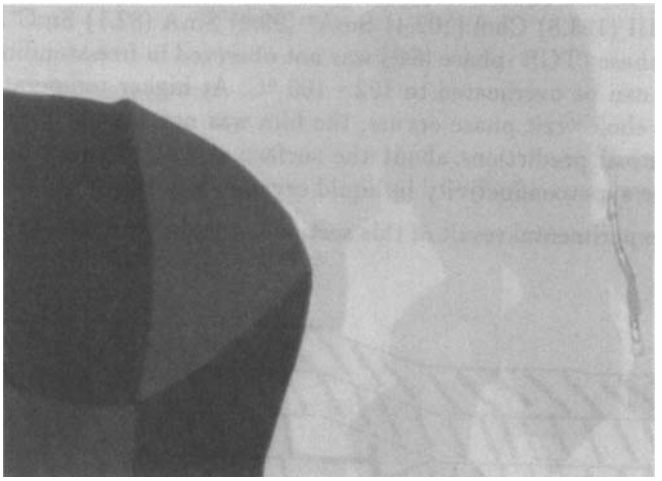

Figure 5. Sm B phase after the transition from Sm F on heating: thick smectic B domains are connected via ultrathin smectic F junctions. See Color Plate XV.

large smectic B domains of initial thickness, which are connected together by much thinner dark or gray pores. After heating to the smectic C phase the dark pores spread over the whole film, because the surface tension decreases with decreasing the number of layers [13]. Reflectivity measurements in the smectic C has given that number of layers in dark pores is always less than 20. According to the phase diagram of figure 3 the pores have smectic F structure.

Thicker steps occur in the inner part of the film as edge dislocations (figure 6a), which correlates to observations of [68]. The cross-section of the film of figure 5 is displayed on figure 6b. The smectic film is mechanically stable because of continuous smectic F layers going over the whole film boundary. Discussed phenomena are very

close to the problem of surface freezing in liquid crystals observed in many experimental situations. Quantized layer growth was found in high resolution synchrotron measurements on the free surface of the isotropic liquid of dodecylcyanobiphenyl (12CB) in [59]. The first smectic layer has been registered at approximatelly 10 °C above the isotropic - smectic A phase transition. Analogous behaviour was observed for isotropic-nematic phase transition [60, 61]. Positional order corresponding to several smectic A layers on the boundary [62] occurs in the nematic phase above the nematic - smectic A phase transition. In free standing films the existence of surface hexatic smectic I layers on the smectic C films has been reported in [63].

4.2 Destruction of the first order Sm A - Sm C* phase transition

The disappearance of the first order phase transition smectic A-smectic C* in free standing films by diminishing the number of layers has been observed in [58, 44].

A ferroelectric material ALLO-902C13M5T have been investigated in [44]. The phase sequence of liquid-crystalline phases for bulky samples (on cooling):
I (126.0) BPI,II,III (123.8) Chol (102.4) SmA* (99.2) SmA (82.1) SmC*.
The smectic A* phase (TGB -phase [64]) was not observed in free standing films: the smectic A phase can be overheated to 102 - 103 °C. At higher temperatures, where transition to the cholesteric phase occurs, the film was not stable. This fact can be refered to theoretical predictions about the surface stabilized smectic A phase - a new analog of the superconductivity in liquid crystals [65, 66].

The main experimental result of this section is the destruction of the first order

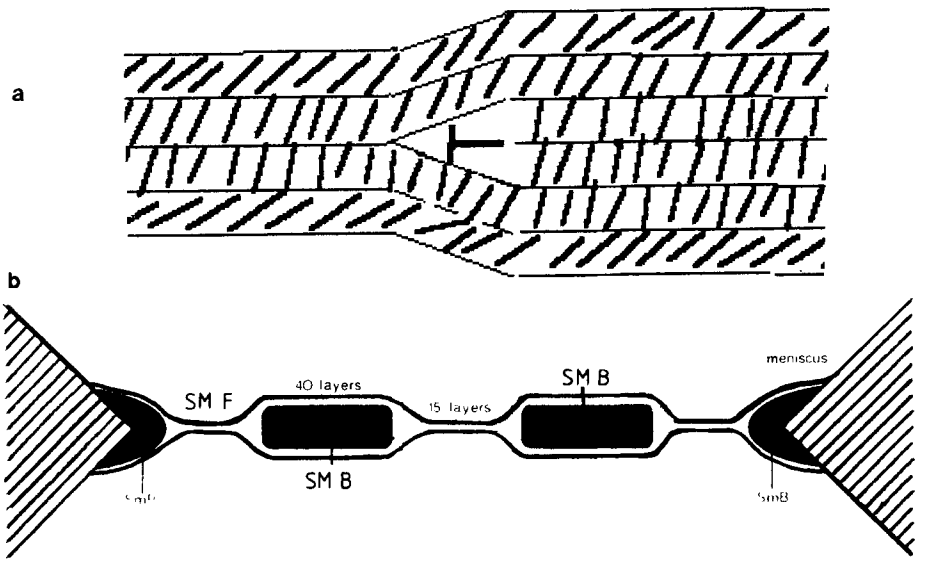

Figure 6. Film cross-section : (a) a step in a film; (b) scheme of the film of figure 5.

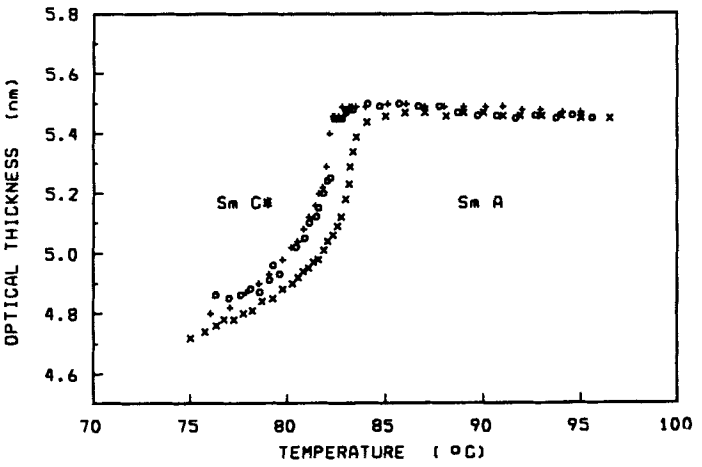

Figure 7. Temperature dependence of the optical density per one layer for 80 (×), 126 (+) and 480 layer (o) films.

phase transition by decreasing the number of layers. The critical number of layers was found by measurements of the optical thickness jump at the phase transition temperature. The critical number of layers was found to be $N_c = 90$. Near the critical point the interphase smectic A - smectic C* boundary disappears. The state of the system changes contineously from the SmA -like to the SmC* in films thiner than N_c. Figure 7 shows the temperature dependence of the optical thickness per one layer for 80-, 126-, and 480- layer films. The curves for $N \geq N_c$ are discontinuous indicating the first order SmA-SmC^* phase transition. The optical thickness variation in the N=80 layer film is continuous. There is no additional rounding of curves in the 80-layer film as compared to bulky 480-layer film. The transition temperature shift for $N \geq N_c$ is negligible. The effect of rounding of d(T) curves was observed in films with $N \leq 70$ layers. Figure 8 shows dependence of the SmA-SmC* phase transition temperature on the number of layers. The solid line corresponds to $N \geq N_c$ and the dotted line to the shifting of the inflexion temperature of the dependences d(T). The inflexion point shifts by approximatelly 4°C to higher temperatures by changing the film thickness from 70 to 10 layers. The critical thickness N_c=15 for the phase transition Sm A - Sm C* has been found in [72] for the ferroelectric compound C7 (see section 5).

The problem of the first order phase transition destruction for the q=3 Potts model by dimensional crossover has been theoretically studied in [67]. In [68] the disappearance of the first order phase transition by decreasing the number of layers was considered as an analogy for the disappearance of the same transition by the application of an electric field [69].

4.3 Numerical simulation of surface ordering effects

In [70] a continuum mean field description of the first order phase transition smectic A - smectic C* in the free standing films analogous to [68] has been used. The state of the film was characterized by a dependence of the tilt angle (Θ) on the coordinate (z) perpendicular to the smectic planes (figure 1). The origin of coordinates has been taken at one of the boundaries. To find the profiles of the tilt angle we have numerically minimized the free energy of the film taken it in a form commonly used for the description of the phase transition smectic A-smectic C* [71]:

$$F = \int_0^L F_c dz \tag{17}$$

where l is the thickness of the film and F_c is the part of the free energy density per unit area of the film coupled with the tilt of the director. The tilt angle was used as an order parameter. The free energy density F_c is given by the following expression:

$$F_c = \frac{a}{2}\Theta^2 + \frac{b}{4}\Theta^4 + \frac{c}{6}\Theta^6 + \frac{g}{2}\left(\frac{d\Theta}{dz}\right)^2, \tag{18}$$

where $a = \alpha\frac{T-T^*}{T^*}$, α is a temperature independent constant and T^* is the temperature of the absolute instability of the smectic A phase with respect to the smectic C* phase. Minimization of the free energy with respect to Θ results in the following differential equation for the function $\Theta(z)$:

$$g\frac{d^2\Theta}{dz^2} + a\Theta + b\Theta^3 + c\Theta^5 = 0 \tag{19}$$

There are two additional boundary conditions, which are sufficient to solve the equation 19:

$$\Theta(0) = \Theta_0 \quad \text{at the surface of the film} \tag{20}$$

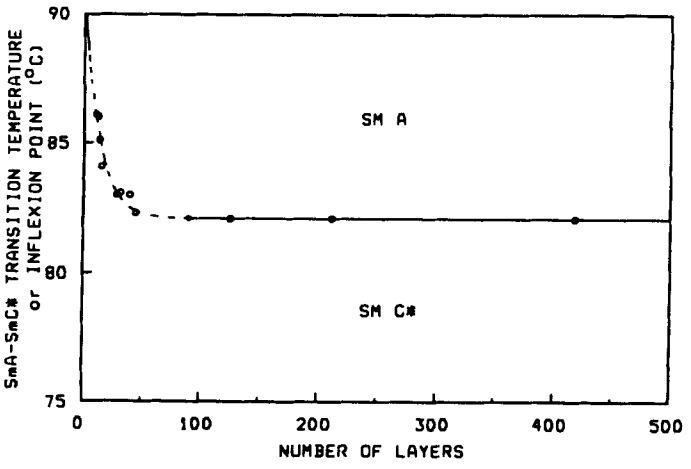

Figure 8. Number of layers dependence of SmA-SmC* transition temperature in ALLO.

$$\left(\frac{d\Theta}{dz}\right)_{\frac{L}{2}} = 0 \quad \text{in the middle of the film} \tag{21}$$

The first boundary condition models the strong anchoring.
To find reasonable numerical solutions by a simulation procedure we used the coefficients α, b, c and g which were calculated from the typical values of the following parameters: $(T_c - T^*)$, where T_c is the first order phase transition temperature; the tilt angle Θ_c at the transition temperature smectic A - smectic C*; the penetration length ξ_0 of the surface induced order and the transition enthalpy ΔH.

The shift of the first order phase transition temperature (T_c) with respect to the absolute instability temperature of the smectic A phase (T^*) can be expressed by:

$$\Delta T = T_c - T^* = \frac{3 \mid b \mid^2 T_c}{16\alpha c}; \tag{22}$$

the tilt angle at the transition temperature Θ_c can be written as:

$$\Theta_c^2 = \frac{3 \mid b \mid}{4c}; \tag{23}$$

In a first approximation the variation of the tilt angle in the boundary region can be described by an exponential function of z:

$$\Theta(z) = \Theta_b + (\Theta_0 - \Theta_b) exp(-z/\xi_0), \tag{24}$$

where Θ_b is the value of the tilt far away from the boundary. ξ_0 is given by:

$$\xi_0 = (\frac{4gc}{3b^2})^{1/2} \tag{25}$$

Values of the transition enthalpy has been taken from [72, 73]. Numerical parameters used in the simulation procedure are summarized as follows:

$\alpha = 6.1 \cdot 10^6 Jm^{-3}$	$T^* = 300K$
$b = -0.75 \cdot 10^6 Jm^{-3}$	$T_c = 301.17K$
$c = 4.4 \cdot 10^6 Jm^{-3}$	$\Theta_c = 20^o$
$g = 6 \cdot 10^{-12} Jm^{-1}$	$\xi_0 = 8nm$
$\Theta_0 = 40^o$	$\Delta H(bulk) = 4 \cdot 10^5 Jm^{-3}$

The fifth parameter of the numerical procedure was the boundary condition for Θ. We report in this paper a more simple case of the temperature independent boundary conditions, therefore we have taken the tilt angle on the boundary to be a constant $\Theta_0 \geq \Theta_c$. Numerical procedure with temperature dependent boundary conditions is now in progress. Differential equation 19 was solved according to a numerical procedure described in [74].

4.3.1 Profiles of the tilt angle

Profiles of the tilt angle calculated for one half of the sample for three film-thicknesses (400 nm, 160 nm, 70 nm) are shown in figures 9 - 11. All plots correspond to the minimum of the free energy eqn. (17) (the stable solutions). In the simulation procedure

the boundary conditions for the tilt angle were kept constant for all temperatures and thicknesses.

Although continuous model was applied, sometimes we shall use "layers" 3.5 nm in thickness (see [44]) to illustrate the relevance of the computer simulation results to known experiments.

The simulation results for a 400 nm film are shown in figure 9. In the smectic A phase the tilt angle descreases abruptly in 3-4 layers starting from a value of Θ_0 to $\Theta = 0$ in the middle of the film. The penetration length ξ_0 is independent on the film thickness and temperature far from the transition. The z-dependence of the tilt angle has no peculiar points (figure 9, T= 312.34 and 302.84 K).

In the smectic C* stability temperature interval the tilt angle varies from Θ_0 to a nonzero temperature dependent asymptotic bulk value (figure 9, T=301.2 K and 296.67 K). In this case the phase transition is abrupt and the profile changes from the smectic A to the smectic C* inside of several tenths of degree. The phase transition temperature is a function of the number of layers and is shifted by approximatelly 1.6 K to the higher temperatures in the 70 layer film with respect to the bulk. An interesting feature of the 400 nm film in the vicinity of the transition temperature is a "surface phase transition" in the smectic A boundary region of approximately 8 layers in thickness (T=301.28 K curve on figure 9). The dependence of the tilt angle on z-coordinate possesses in this case has two inflexion points which is qualitatively different to the curves at all other temperatures. The change of the Θ profiles with temperature indicates that the phase transition smectic A-smectic C* is a discontinuous one. By definition the first order phase transition takes place at the temperature where the tilt angle profile with two inflection points transforms to the monotoneous smectic C* profile.

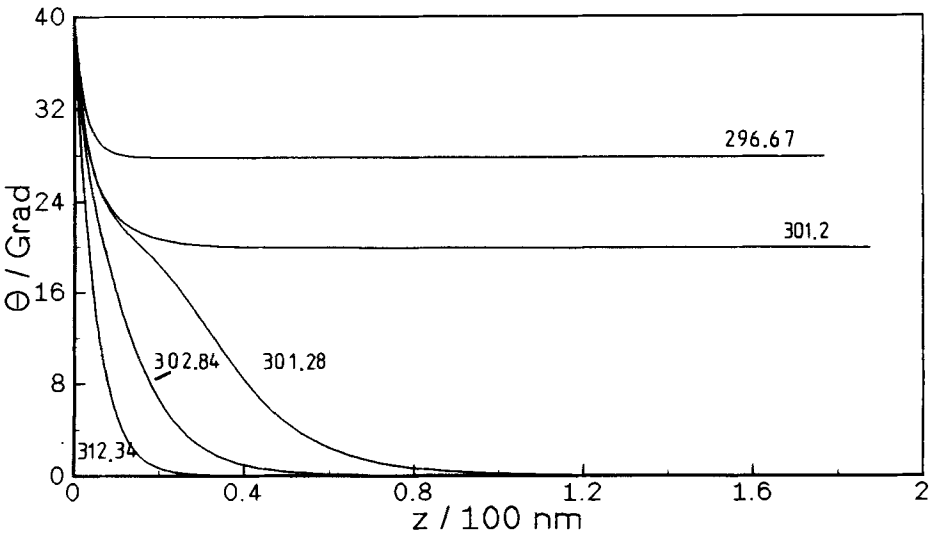

Figure 9. Tilt angle profiles in a 400 nm film at different temperatures. The first order phase transition Sm A/Sm C* occurs at $T_c \approx 301.2K$.

The simulation results for a 160 nm and 70 nm films in figure 10 and 11 show that the transition temperature increases and the temperature interval where the profile varies from the smectic A to the smectic C* becomes broader by decreasing the number of layers. In the vicinity of the critical thickness the tilt angle profile essentially depends on the film thickness. The "boundaries" of the smectic C* surface region at T=301.46 K in figure 10 are practically not observable, but the main feature of this state (two inflexion points) remains unchanged. In a 70 nm film (figure 11) the tilt angle profiles with two inflection points were not found and the phase transition disappears. The state of this film is continuously changed from the smectic A -like to the smectic C*-like by decreasing the temperature. For films thiner than 70 nm no qualitative changes of the temperature dependence of the tilt angle profiles were observed. It is important to emphasize that the critical film thickness where this behaviour occurs first is about one order of magnitude larger than the penetration length ξ_0. This is a nontrivial result, because from a naive point of view one could expect that the thickness where the first order phase transition smectic A - smectic C* disappears should be approximatelly equal to $2\xi_0$. Our simulation describes a qualitatively different behaviour and demonstrates the importance of the tails of the $\Theta(z)$ profiles far from the boundary. Let us compare our simulation results with the experiments reported in [58, 44]. Authors of [58] have measured the average tilt angle in free standing films as a function of temperature and number of layers. In [44] the optical thickness of films has been determined which gives an average value of $\cos(\Theta(z))$, if one neglects the temperature dependence of the refractive index. The critical thickness in [58] was approximatelly 52 nm and in [44] 315 nm.

Figure 12 shows calculated temperature dependence of $< \cos\Theta >$ for different film thicknesses. In the thick films this value reveal a discontinuity at the phase transition temperature. In a 70 nm film the discontinuity disappears. Our calculations give a critical thickness, which qualitatively corresponds to the results of [58]. An

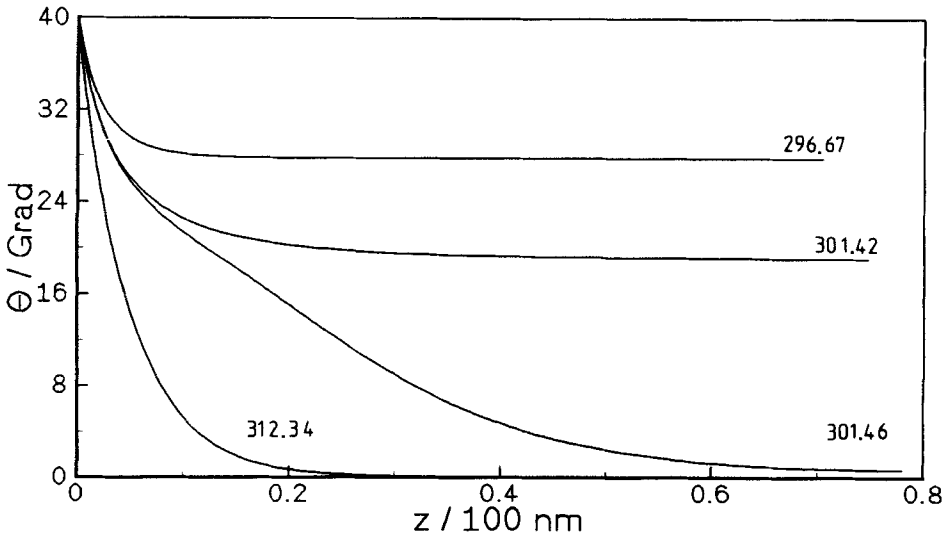

Figure 10. Tilt angle profiles in a 160 nm film; $T_c \approx 301.4K$.

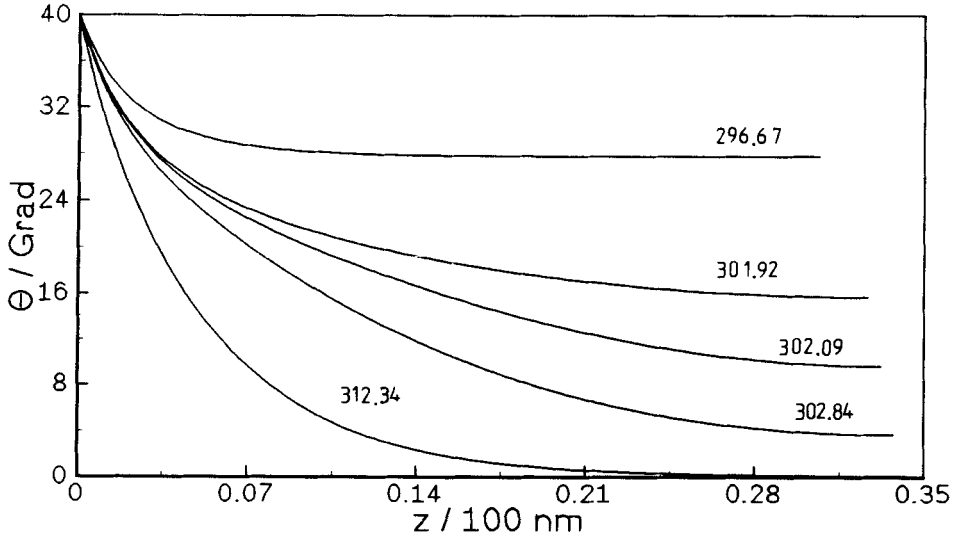

Figure 11. Tilt angle profiles in a 70 nm film. The phase transition smectic A - smectic C* disappears in this film.

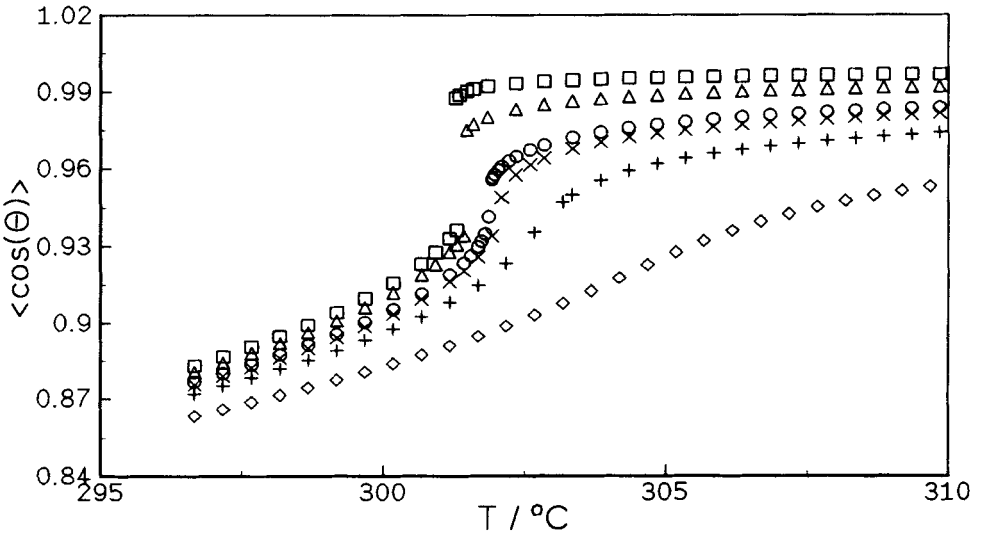

Figure 12. Temperature dependence of $< \cos\Theta >$ for film thicknesses: 400 nm (□), 160 nm (△), 80 nm (○), 70 nm (×), 50 nm (+) and 30 nm (◇).

increase of the penetration length in the numerical procedure led to an increase of the critical thickness. Thus, the different critical thicknesses found in [58] and [44] can be explained by different penetration lengths of the surface order at the boundary liquid crystal - air. It is interesting to point out that the critical thickness found in the calculations of figure 12 coincides with that of figures 9 - 11, although the definition of the transition temperatures is different. To obtain a quantitative description

of the experiments of [58, 44] the values of the Landau expansion coefficients must be known.

4.3.2 Free energy density

A study of the temperature dependence of the free energy density gives an important information about the change of the character of the phase transition caused by a decrease of the film thickness. From the general theory of the first order transition [75] it is well known, that the free energy can be described by a double well function of the oder parameter in the vicinity of the phase transition temperature. The local minima correspond to the coexisting phases (in our case the smectic A and C*). At a certain temperature T** above the phase transition the Sm C* minimum disappears. The lower boundary of the temperature interval where the free energy exhibits two local minima is noted by T*. At this temperature the Sm A minimum disappears. The free energy of the system varies continuously at the transition point [75], therefore the condition for the phase transition is given by:

$$F_A = F_{C^*} \tag{26}$$

The disappearence of the phase transition is qualitatively illustrated in figure 13 where the free energy density is shown as a function of the average tilt angle and the film thickness at the transition temperature. The smectic A and smectic C* states are separated by an energy barier. The energy barrier decreases and both minima approach to each other by a decrease of the number of layers. At the critical thickness any difference between above mentioned states disappears. Surface or-

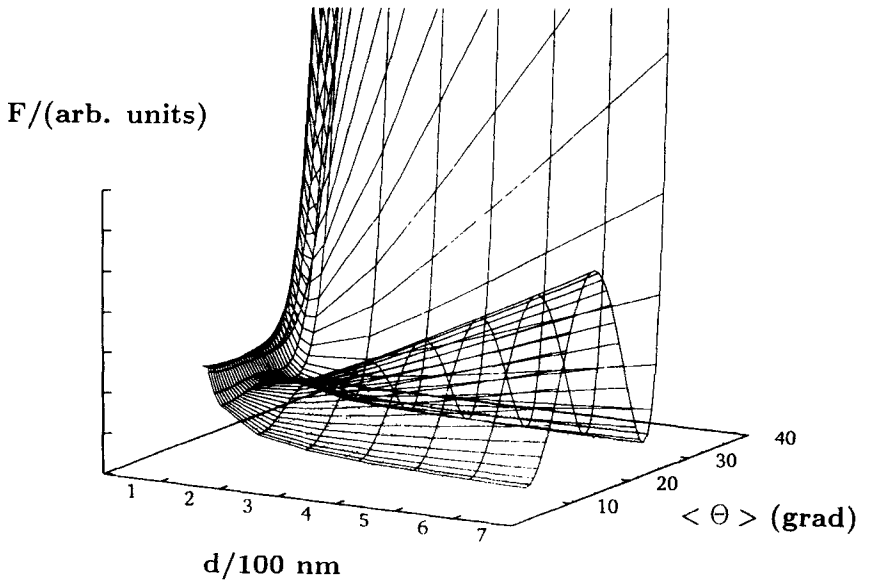

Figure 13. Free energy as a function of film thickness and the average tilt angle $< \Theta >$.

dering effects in free standing films are described using a computer simulation based on the Landau theory with strong boundary conditions. By the decrease of the number of layers the phase transition smears out, the transition temperature is shifted to higher temperatures and the discontinuities of the integral structural parameters $< \Theta >$ and $< \cos\Theta >$ as well as the energy barrier between smectic A and smectic C* phases become smaller.

The first order phase transition smectic A-smectic C* disappears at some critical thickness which depends on the coefficients of the Landau expansion, especially on the value of the parameter g. A nontrivial result of this paper is that the critical thickness is approximatelly one order of magnitude larger than the penetration length ξ_0 of the surface order characterizing the variation of the tilt angle from its value at the boundary (Θ_0) to the bulk (Θ_b). In films thinner than the critical thickness all average structural parameters and the first derivative of the free energy become continuous functions of temperature, the energy barier between the smectic A and smectic C* phases and the surface phase transition disappear. The computer simulation results describe qualitatively correct recent experimental results [58, 44].

This problem can be treated qualitatively using approximate analitical results of [68]. Because of the dependence of Θ on vertical coordinate z, each layer has own transition temperature. Now let us consider the free energy density in the middle of the film and use the approximate solution (20) for z=L/2. We obtain

$$\begin{aligned} F_{z=d/2} &= \frac{g}{2\xi_0^2}(\Theta_0 - \Theta)^2 exp(-L/\xi_0) + (1/2)a\Theta^2 - (1/4)b_0\Theta^4 + \\ &+ (1/6)c\Theta^6 = (1/2)\alpha(T - T_c^* - \Delta T_c)/T_c^*\Theta^2 - \\ &- (1/4)b_0\Theta^4 + (1/6)c\Theta^6 - E_{eff}\Theta \end{aligned} \tag{27}$$

with

$$\Delta T_c = T_c^* \frac{g}{2\xi_0^2 \alpha} exp(-L/2\xi_0) \tag{28}$$

and

$$E_{eff} = \frac{g}{2\xi_0^2}\Theta exp(-L/2\xi_0) \tag{29}$$

The influence of the both boundaries is equivalent to the transition temperature shift in the middle of the film ΔT under the action of an effective external field E_{eff} given by equation (29). This field is exponentially decaing when the film thickness is increased and appears to be important only when the thickness L is of the order of ξ_0. Thus we have approximatelly reduced the problem to the well known question about the first order transition in the external field. This problem has been considered by many authors and corresponding solutions for the tilt angle as a function of the temperature and the external field can be found in [69, 76]. Using expression (28) we have fitted the dependence of the inflexion point on the number of layers on the figure 8 for $N \leq N_c$. The fitting curve with parameters ξ_0=7.1nm and g/α=2.6 nm^2 is shown with a doted line.

Computer simulation results show that temperature dependences of the tilt angle and the average interlayer spacing can be described by taking into account the ordering effects on the film boundary. The shifting of the transition temperature

and the smearing of the pretransition characteristics for $N \geq N_c$ have not been experimentally found for ALLO. Results of [58] on the contrary give evidence for such effects. This discrepance can be explained by ferroelectricity effects on the phase transition in C7 discussed below. In the case of ALLO [44] the transition enhalpy for the transition Sm A - Sm C* is smaller than in C7. Therefore, one can expect more pronounced finite-size scaling effects. But this is not the case here, although the critical thickness in ALLO is 6 times larger. This contradiction is an indirect argument for the importance of the surface ordering phenomena in the destruction of the first order phase transition Sm A- Sm C*.

5 Stable configurations of the 2D director field in ferroelectric free standing films with high spontaneous polarization

Surprisingly, ferroelectric properties in two dimensions stood outside of researchers attention for a long period of time and the first experimental works appeared only recently [82]. The main reason for this omission was that materials with high spontaneous polarization became available only in the late 80's [72]. Free standing films provide new experimental possibilities for study of thermodynamically stable structures in smectic phases, because rotation of the director around the layer normal is no more limited by the boundary conditions and weak molecular interactions suppressed by the influence of the substrate can reveal themself.

Properties of ferroelectric films with high spontaneous polarization are qualitatively different with respect to non-ferroelectric films. (4- (3 - methyl - 2- chloropentanoyloxy) - 4' heptyloxybiphenyl) (C7) and its chiral - racemic mixtures have been studied in this paper. C7 possesses the following sequence of liquid-crystalline

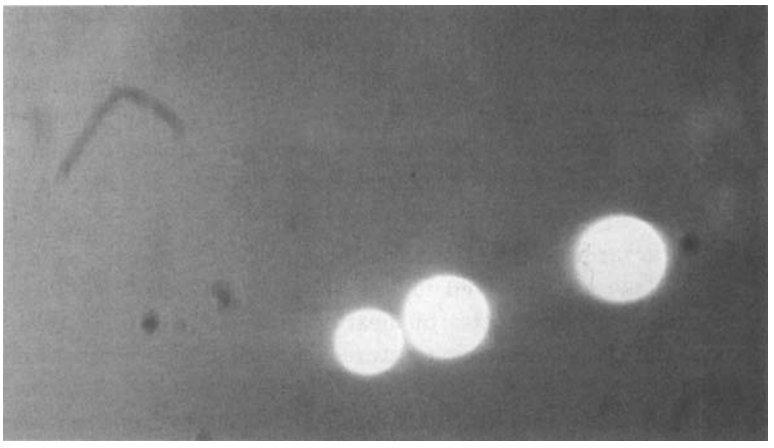

Figure 14. Spontaneous growth of thicker islands in a N=15 smectic C* film of C7. See Color Plate XVI.

Figure 15. Flow of the substance from the meniscus into the film after the phase transition Sm C_A - Sm C^* in N≈15 film of Y1. See Color Plate XVII.

phases: isotropic (62°C) smectic A (54.6 °C) smectic C* (43°C) smectic G.

Spontaneous polarization in the smectic C* phase of pure C7 varies between 130 and 290 nC/cm^2 with decreasing temperature. The coexistence region of the C7 racemic mixture was 0.3 $^\circ C$. According to [13] the surface tension descreases with decrease of number of layers. This is not true for the ferroelectric films. Figure 14 shows a spontaneous growth of a N≈30 island in a 15 layer film of the smectic C* phase of the 75% mixture of C7 with its racemat. The dark part of the film possesses a homogeneous anisotropic structure discussed below. A singular point is located in the center of the thicker island and the director field forms a circular configuration around this point.

Second example of unusual behaviour of the high spontaneous polarization films was observed in the ultrathin films of 4-(2-methyloctanoyl) phenyl-4' -octyloxybiphenyl-4-carboxylate (Y1) (figure 15). This substance has the following liquid-crystalline phases sequence: isotropic (153.8) smectic A (135.3) smectic C* (ferroelectric) (79) smectic C_A (antiferroelectric) (50.3) smectic X (31.2) cryst [77]. After the phase transition smectic C_A - smectic C* in N=15-20 films the substance begins to flow from the meniscus into the film and it spontaneously becomes thicker. In films with a low spontaneous polarization an opposite behaviour is typical.

Two novel structure modifications of the smectic C* phase: an anisotropic state and a stripe state are observed in free standing ferroelectric films [78]-[80]. Transformations between these states on heating and cooling are reversible. N/T phase diagrams of the chiral - racemic mixtures show that the stripe state is stable only in high spontaneous polarization mixtures. Figure 16 shows N/T phase diagram of the smectic C* structural modifications in C7. Two states has been observed in thick films ($N \geq 85$). An anisotropic state occurs close below the phase transition Sm A - Sm C* after the relaxation of defects. This state is characterized by a homogeneous contrast between crossed polarizers, which is changed by the rotation

of the microscope table (figure 17). A stable stripe state occured spontaneously in thick films ($N \geq 85$) on cooling at a temperature (T_s) below the Sm A - Sm C* phase transition. The dependence of T_s on the number of layers is shown on figure 16. The structure transformation anisotropic - stripe state is reversible: the stripe state disappears on heating 1-3°C above T_s. This behaviour is reminiscent to the hysteresis of structural transformations at the first order phase transition. The best way to register the stripe state is to follow the stripe formation process at the film contour. Prolongated stripe sources 100-200 μm in length occur near T_s and produce stripes, when T_s is reached. Interaction of stripes of different sources results in a typical texture, which is called here a striped state. Normaly the stripe texture is deformed and it is dificult to ascribe some characteristic periodicity to it. Typical periodicity of this state is relatively large (~80-150μm). Figure 18 shows a typical stripe state near a source in a 420-layer film at T=49.5 °C. The stripe texture can be deformed and aligned by the motion of the movable side of the film frame. In this case stripes are oriented parallel to the edges of the frame.

The anisotropic state temperature interval increases with decreasing the number of layers. At $N_c \approx 85 \pm 10$ the stripe state of pure C7 disappears. The relaxed structure in ultrathin films ($N \leq 30$) is also anisotropic. One of possible configurations of the director field is the 'chess-board' texture, observed in [78]. However we have not succeded to produce this texture on whole film area. The anisotropic relaxed structures in thick and thin films can not be distinguished in the optical microscope. Difference between the relaxed textures of the anisotropic state in thick and ultrathin films is related to the structure of defects. Discontinuous defect walls (figure 19) are typical for notrelaxed in ultrathin films ($N \leq 30$). Relaxation of these walls is a very slow process and the texture of figure 19 is quasistable. Defect-free ultrathin films have been produced from very thick films by successive removing of smectic layers during 2-3 hours. During this process each film has been cooled to the smectic C* phase and annealed during 10-15 minutes. Variation of contrast in the

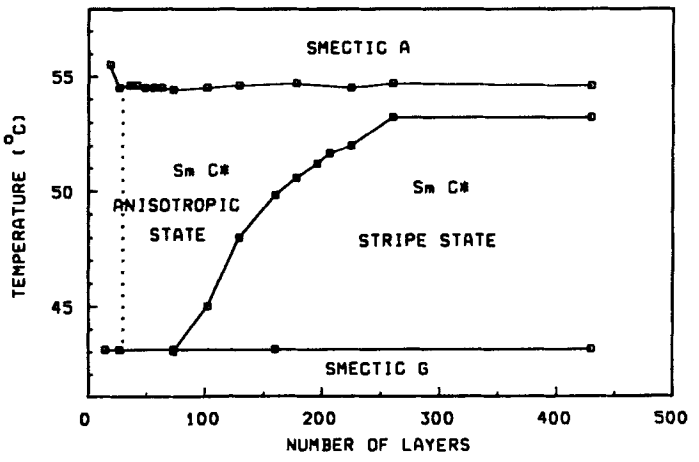

Figure 16. N/T phase diagram of C7.

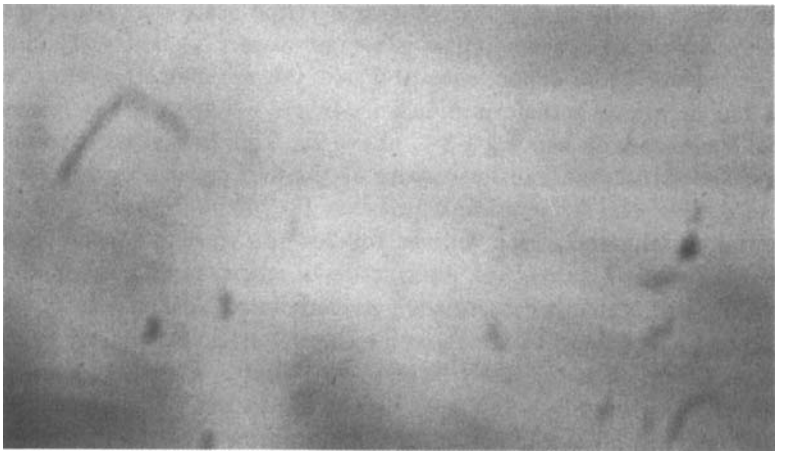

Figure 17. Relaxed anisotropic state in 25 -layer film at T=48.06°C. See Color Plate XVIII.

anisotropic state in thick films was always smooth. Relaxation time for the anisotropic state was about half an hour in thick films. Pseudostripes, produced by motions of point defects have been observed in thick films in the temperature interval of the anisotropic state. Such stripes can be topologically stable, when the point defects move from one side on the film contour to the other, but not reproducible and have not filled the whole film area.

It was found that the striped state completely disappears in chiral - racemic mixtures with concentration of chiral C7 less than 75%. Figure 20 shows the shift of T_s with respect to T_{AC^*} on number of layers for mixtures with 100, 92.5, 87.5 and 85 wt. % chiral C7. The anisotropic state with discontinuous walls has been found in mixtures with more than 95 % of chiral C7. In 50% mixture of C7 no textural

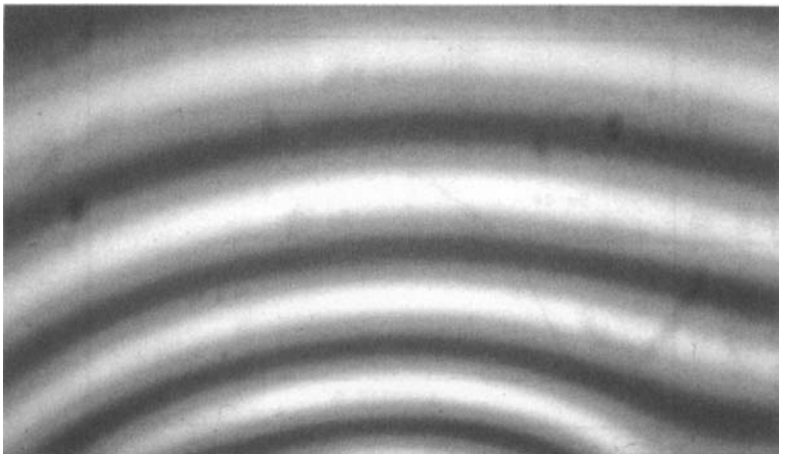

Figure 18. Stripe state near a source on 420-layer C7 film contour at T=49.5°C. See Color Plate XIX.

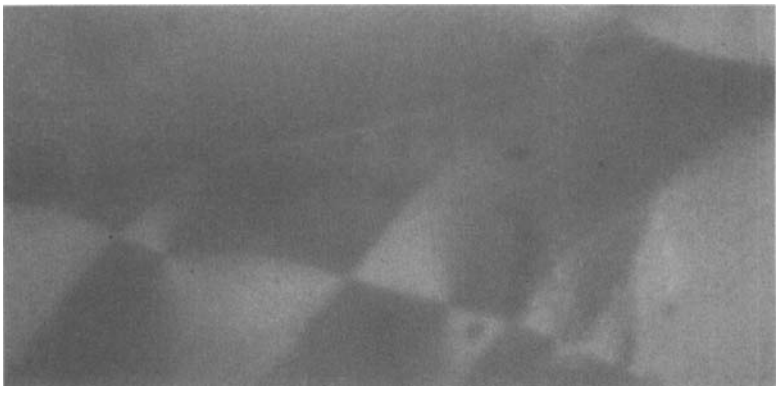

Figure 19. Notrelaxed anisotropic textures of the smectic C* phase in N=20 film at T=49.96 °C. See Color Plate XX.

changes has been observed in the smectic C* by decreasing the temperature. The stable texture of this mixture is similar with the schlieren texture of the nematic phase. The texture of the anisotropic state in thick films transforms continuously in a schlieren texture of C7 racemat by decreasing the concentration of chiral C7. Figure 21 shows a texture of a 150-layer film of a mixture of 87.5 % C7 with its racemat at T=53.85°C. Details of these measurements will be published elsewhere.

The influence of the dipolar interaction on the smectic C* structure in the free standing films can be characterized by L_g [33]. Let us estimate this value using expression (10). Taking K≈ 10^{-6}dyn and the value of P from the experimental data of ref. [72], one obtains $L_g \approx 100$ nm, the layer thickness in the smectic A phase taken from [58] is d=2.47 nm. Therefore the critical thickness is expected to be 40 layers. This estimation correlates very well with the experimentally found value for

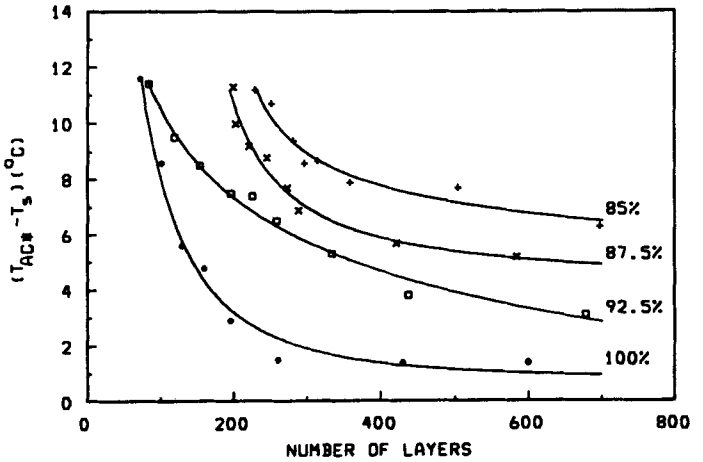

Figure 20. Dependence of the transition temperature anisotropic - stripe states on the C7 concentration. Solid curves in each case are eyes guides.

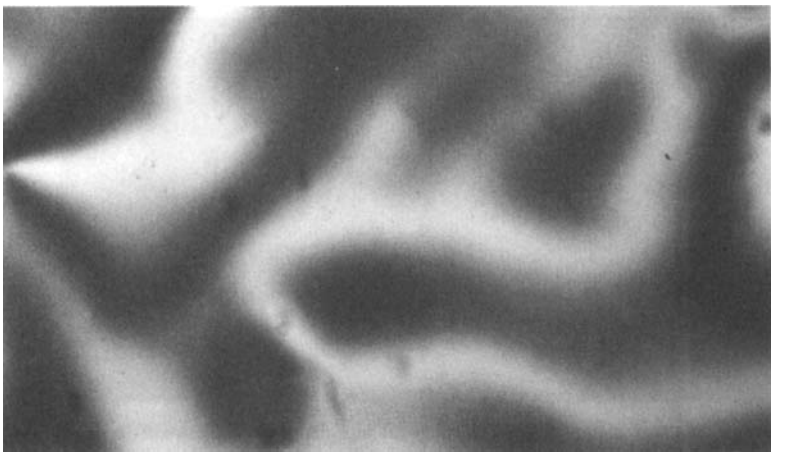

Figure 21. Anisotropic texture of the smectic C* phase in a mixture of 87.5% C7 with racemat, N=150, T=53.85 ^{o}C. See Color Plate XXI.

occurence of the anisotropic state with discontinuous walls $N_c \approx 30$. Anisotropic state in thicker films and in mixtures with lower C7 concentration can correspond in the framework of this model to the orientationally disordered state with an algebraic decay of order, described in [33, 34]. To distinguish between these two states other techniques should be applied, which is now in progress.

The stripe state is observed only in thick films ($N \geq 85$), therefore it can be regarded as bulky stable structure in samples with free boundaries. The absence of boundary conditions for the asimuthal angle of the director in free standing films is one of the important reasons for their formation. The current work shows, that the stripe state stability is combined with the high spontaneous polarization of the substance. This result exludes the elastic mechanism of the stripe formation in the form proposed in [17]-[19].

In [81] a new mechanism of the stripe formation has been discussed, which can be relevant to the present studies. Using the Landau expansion it was shown that in substances with a large value of the flexoelectric coefficient μ [71] spatial modulations of the polarization can spontaneously occur. Modulations with rotation of the director parallel and perpendicular to the smectic planes are considered.

Flexoelectricity can influence structures of the smectic C* phase in the other way. It is known, that elastic coefficients [71] depend on the value of flexoelectric coefficient. The particular form of this dependence in free standing films with high spontaneous polarization has not been investigated. The Frank elastic coefficients can be changed so, that the elastic mechanism of [17] - [19] will work. To answer, what mechanism function in reality, measurements of elastic coefficients in chiral-racemic mixures of C7 are necessary.

6 Surface tension effects

6.1 Transient phases induced by surface tension change

Because the surface - volume ratio in free standing films is large, strong influence of the surface tension on smectic phases structure can be expected. On the other hand, surface energy correlates with the structure of the boundary layers. For free standing films the surface tension is a new thermodynamic parameter analogous to pressure, which determines conditions for the phase equilibrium. As it was shown in [73] transient phases can be induced by surface tension change. Free standing smectic films are practically the only object of confined dimension, where surface tension effects can be studied on a quantitave level, because the surface tension can be measured with a high precision [13].

Free energy of a free standing film can be written in the form:

$$F = F_{el} + F_P + F_{surf}, \tag{30}$$

where F_{el} is the Frank elastic energy including the term linear in $(\mathbf{c} \cdot curl\mathbf{c})$; F_P is a sum of contributions combined with the dipolar interaction and the flexoelectricity; F_{surf} is the surface free energy.

The last term of eqn.(30) can be expressed in the following form:

$$F_{surf} = N\mu + \alpha\sigma \tag{31}$$

where N is the number of molecules in the film; μ is the chemical potential for molecules on the boundary, σ is the area of the film and $\alpha = \frac{\partial F_{surf}}{\partial \sigma}$ is the surface tension coefficient.

The first thermodynamic condition for the phase coexistence is the equivalence of their chemical potentials. The second condition, lacking in the bulky samples, is the identity of the surface tensions of the coexisting phases [44]. This condition follows from the mechanical equilibrium of the interphase boundary between two phases.

In [83] influence of tension on the first order phase transition smectic F-smectic B (crystalline) in 5O.6 was studied. Surface tension has been changed by an abrupt pulling or pushing the mobile side of the frame. The number of layers during the process of tension variation was constant. After a definite time interval the surface tension change is smoothed out by the diffusion of molecules. The surface tension jump in these conditions is limited, because by very quick variation of the area pores can be born and thickness will be changed. Figure 22 shows the shape of the Sm B domains induced in smectic F phase by pushing a film of 5O.6 at the temperature 0.2°C below the phase transition Sm F-Sm B. The film thickness was aproximatelly 60 layers. The smectic B domains have a romboidal morphology and relax to the uniform smectic F phase with the time constant of 10 sec.

Interesting results were obtained in a series of measurements of eigenfrequency of films vibrations which directly give the surface tension (this method has been developed in [60, 13]). Shortly, in this method vibrations in films are exited by an

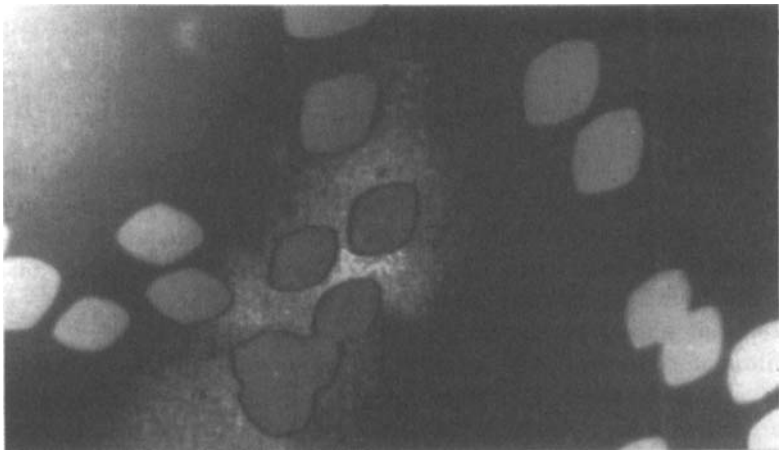

Figure 22. Romboidal single crystals of the smectic B (crystalline) phase induced in smectic F phase close below the phase transition SmF-SmB by an abrupt decreasing of the film area in 5O.6 [83]. See Color Plate XXII.

application of a sinusoidal voltage between the metalic frame and two electrodes positioned directly below the film but without touching it. The intensity of the reflected laser beam was measured by a modulation technique, analogous to figure 2. The exitation frequency was equal to one of the eigenfrequences of the film. The electronic system followed the sygnal frequency and phase after some subtle changes of the film area. The measured eigenfrequency is proportional to the square root of the surface tension [13].

Figure 23 shows time dependence of the signal phase in the smectic F, smectic B phases and the coexistence region after some small and fixed decrease of the film area. The broadeness of this curve gives the relaxation time of surface tension. The difference between initial phase shift (zero) and the asymptotic value is ascribed to the change of the geometrical parameters of the film. The end of the displacement of the movable frame side corresponds to the beginning of the vertical increase of the phase. The relaxation time of tension in the smectic F phase 0.7°C below the phase transition was about two seconds (figure 23a). Microscopic observations show that no smectic B domain have been produced. The relaxation of tension in this case is combined only with the diffusion of molecules from the smectic F phase into the meniscus.

Figure 23b shows the phase relaxation curve 0.2°C below the SmF-SmB phase transition. In this case smectic B domains have been produced after pushing. The measured curve differs qualitatively from figure 23b. One can recognize three different processes. The early process is combined with the film relaxation due to the diffusion of molecules from the smectic F to the meniscus. This process is broken up by the smectic B domains formation, which is chracterized by a longer time constant. The final process is mainly combined with the tension relaxation due to the dissolution of the smectic B domains in the smectic F surrounding.

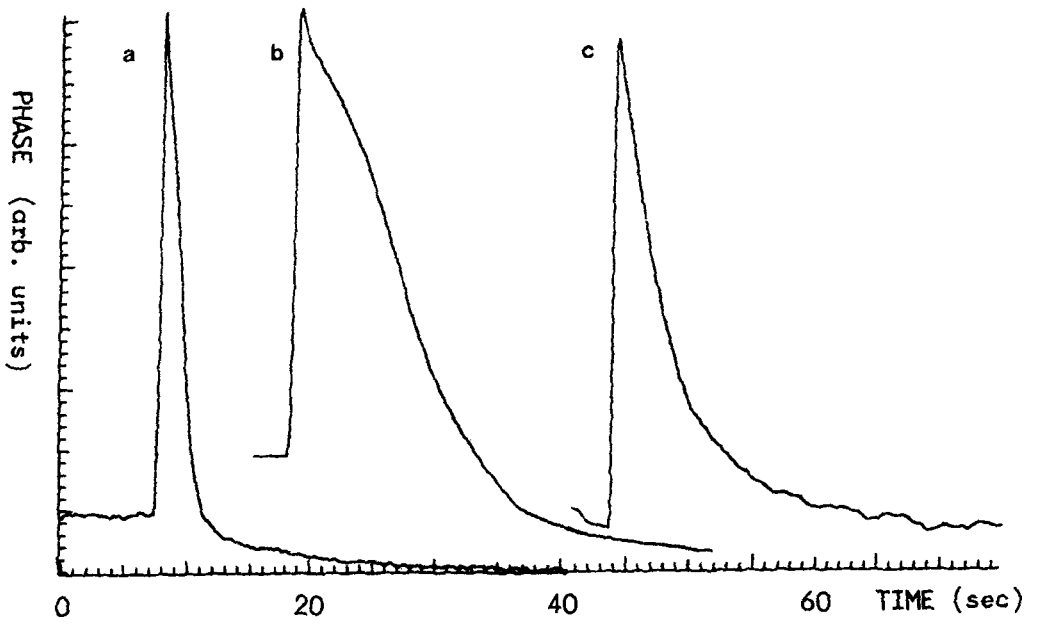

Figure 23. Time dependence of the signal phase after a step-wise displacement of the movable side of the frame in a 56-layer film of 5O.6: a) smectic F at T=39.44 °C (no domains of smectic B phase) ; b) smectic F+ smectic B coexistence region T=40.11°C (the smectic B domain were induced by the change of tension); c) smectic B at T=48.35° [83].

Figure 23c shows the phase relaxation curve for the homogeneous smectic B phase in a film with a constant thickness. The relaxation time was about 4 seconds.

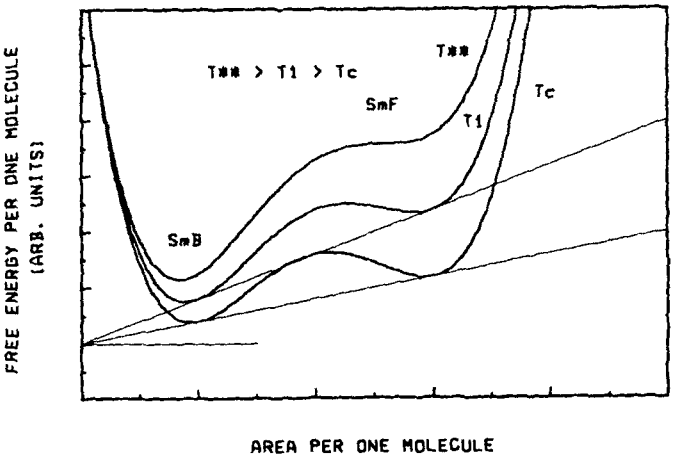

Figure 24. Schematic plot for the free energy per one molecule in the temperature interval between T^* and T^{**} of the phase transition smectic F- smectic B.

This curve was measured after some touch to the frame without any displacement. Because of crystallinity of the smectic B phase the frame displacement results in a large jump of frequency, so that electronic system was not in position to locate the initial eigenmode. The main diffusion process here takes place between the smectic B phase and the meniscus. In the case of large deformations, when the smectic F islands are born the interphase diffusion plays more sufficient role in the relaxation process.

The life time of the transient phases is determined by a competition of the two processes: interphase diffusion and diffusion from meniscus. The free energy of the system has a double-well structure in the vicinity of T_c. Figure 24 shows a tangent construction for the Sm B - Sm F phase transition. The phase transition in free standing films takes place between the states possessing equal slope of $f_N(a)$ equal to the surface tension. An abrupt increase of the surface tension makes the phase equilibrium at higher temperatures possible. According to this model the tension induced phase transitions can be observed only in the temperature interval between T^* and T^{**}. The energy barier between smectic B and F phase disappears at $N \approx 33$. In thick films the energy barier is large enough to prevent the formation of the smectic F after an increase of the surface tension. Analogous consideration can be made for a decrease of surface tension (pushing). This theoretical scheme explains the upper temperature and thickness boundary where the effect can be observed. Generally it also clear that this effect is expected for weak first order phase transitions.

6.2 Correlation between the boundary reconstruction and the surface tension temperature dependence

We have seen that the boundary layers of free standing films in many cases possess different structures with respect to the inner layers. Temperature dependence of the surface tension is related to the structure in surface layers and can be described using the wetting analogy. We shall consider the reconstructed boundary layers as being adsorbed on the surface of a smectic phase from its own vapour. This case is analogous to the formation of a liquid layer condensation on the surface of a solid crystal [15]. γ will denote an average concentration of adsorbed molecules per unit area, which is proportional to the thickness l of the adsorbed film:

$$\gamma = \frac{\rho l}{m}, \tag{32}$$

where m is the molecular mass and ρ is the material density.

The temperature dependence of the surface tension can be described using thermodynamic inequalities obtained in [15]:

$$(\frac{\partial \mu}{\partial \gamma})_T \geq 0 \tag{33}$$

$$(\frac{\partial \alpha}{\partial \gamma})_T \leq 0 \tag{34}$$

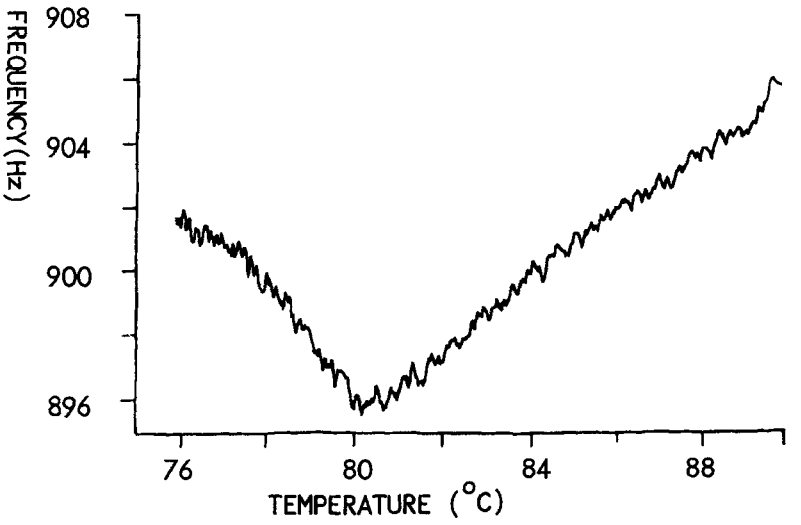

Figure 25. Temperature dependence of the eigenfrequency of the N=101 layer film of ALLO (together with I. Kraus and P. Pieranski).

Because the surface tension coefficient α is only a function of temperature, one can write:

$$\frac{d\alpha}{dT} = (\frac{\partial\alpha}{\partial\gamma})_T \frac{d\gamma}{dT} \tag{35}$$

Possible relations between structures in inner and boundary layers were listed in section 2.3. When the boundary layers have the same structure as the inner layers but different order parameter, the thickness of this layer will decrease or remains constant by decreasing the temperature:

$$\frac{dl}{dt} \sim \frac{d\gamma}{dT} \geq 0 \tag{36}$$

An opposite sign would mean that the surface induced order has an infinite penetration length. This case corresponds in accordance with 34 and 35

$$\frac{d\alpha}{dT} \leq 0 \tag{37}$$

When the surface layers structure is similar to some of low temperature phases $\frac{d\gamma}{dT} \leq 0$, therefore $\frac{d\alpha}{dT} \geq 0$. Such a behaviour has been observed in [83] for the smectic A and smectic C* phases of ALLO, which is shown on the figure 25. The surface ordered layer in the smectic A of ALLO possesses the smectic C* structure and becomes thicker by decreasing the transition temperature. Thus, in the smectic A phase on eshould expect $\frac{d\alpha}{dT} \geq 0$.

Boundary layers in the smectic C* are supposed to have the possess the same structure as the inner layers but a higher order parameter. Experimentally observed slope $\frac{d\alpha}{dT} \leq 0$ correlates with (37).

7 Conclusions

Stable structures in free standing films result from the competition between the thermal fluctuations, which decrease the order parameter, and the surface effects and the dipolar interaction, increasing the average order parameter. Surface ordering effects studied by computer simulation demonstrated a good correlation with experiment. New structural states of the smectic C* were observed in the ferroelectric films with high spontaneous polarization. Using the wetting analogy it was shown that the temperature dependence of the surface tension correlates with the type of surface ordering. As a continuation of this work it is interesting to study the relation between the hexatic order and the chiral in-plane order in hexatic phases with high spontaneous polarization and to check experimentally the universality of the correlations between the type of the surface reconstruction and the surface tension in free standing films.

8 Acknowledgements

Author wish to express his gratitude to Prof. P. Pieranski for the introduction into the subject, I. Kraus for the productive cooperation, to Prof. H. Stegemeyer for his interest to this problem and kind help, to the Alexander von Humboldt Foundation, the Deutsche Forschungsgemeinschaft and the Fonds der Chemischen Industry (Germany) for the financial support of this work.

References

[1] M.E. Fisher, Critical Phenomena ed by M.S. Green (Academic Press, New York), p. 1 (1971).

[2] M.N. Barber, Phase Transitions and Critical Phenomena

[3] K. Binder, Ferroelectrics **73**, 43 (1987).

[4] J.W. Doane, A. Golemme, J.L. West, J.B. Whitehead and B.-G. Wu, Mol. Cryst. Liq. Cryst. **165**, 511 (1988).

[5] D.H. Van Winkle and N.A. Clark, Phys. Rev. Letters **48**, 1407 (1982).

[6] M. Gharbia, A. Gharbi, M. Cagnon and G. Durand, J. Phys. France **51**, 1355 (1990).

[7] H. Rehage and A. Burger, Physica A **194**, 424 (1993).

[8] C.Young, R.Pindak, N.A.Clark and R.B.Meyer, Phys. Rev. Lett. **40** , 773 (1978).

[9] C. Rosenblatt, R. Pindak, N. Clark and R.B. Meyer, Phys. Rev. Lett **42**, 1220 (1979).

[10] C.Rosenblatt, R.B.Meyer, R.Pindak and N.A.Clark, Phys. Rev. A bf 21, 140 (1980).

[11] R.Pindak, C.Young, R.B.Meyer and N.A.Clark, Phys. Rev. Lett. **45**, 1193 (1980).

[12] J.D. Brock, R.J. Birgenau, J.D. Litster and A. Aharony, Contemp. Physics **30** 321 (1989).

[13] P.Pieranski et al., Physica A, **194**, 364 (1993).

[14] C.C. Huang and T. Stoebe, Adv. in Physics **42**, 343 (1993).

[15] L.D. Landau, Collected papers ,(Gordon and Breach, New York) p. 210 (1967); L.D. Landau and E. M. Lifshits, Statistical physics,(Oxford, Pergamon Press 1959).

[16] R. Holyst, Phys. Rev. **44A**, 3692 (1991).

[17] P.G. de Gennes, The physics of liquid crystals, (Claredon, Oxford, 1974), p.125, p.311.

[18] S.A.Langer and J.P.Sethna, Phys. Rev. A ,**34** (1986), 5035.

[19] G.A.Hinshaw, R.G.Petschek and R.A. Pelcovits, Phys. Rev. Lett., **60** (1988), 1864.

[20] R.J. Birgenau, J.D. Litster, J. Phys. Lett.(Paris) **38**, 1399 (1978).

[21] B.I. Halperin and D.R. Nelson, Phys. Rev. Lett. **41**, 121 (1978).

[22] D.R. Nelson and B.I. Halperin, Phys. Rev **B19**, 2457 (1979).

[23] D.E. Moncton and R. Pindak, Phys. Rev Lett. **43**, 701 (1979).

[24] R. Pindak, D.E. Monkton, S.C. Davey and J.W. Goodby, Phys. Rev. Lett. **49**, 1135 (1981).

[25] S.B. Dierker, R. Pindak and R.B. Meyer, Phys. Rev. Lett. **56**, 1819 (1987).

[26] J.D. Brock, A. Acharony, R.J. Birgenau, K.L. Evans-Lutterodt, J.D. Litster, P.M. Horn and J.C. Liang, Phys. Rev. Lett. **57**, 98 (1986).

[27] J.D. Brock, D.Y. Noh, B.R. McClain, J.D. Litster, R.J. Birgenau, A. Acharony, P.M. Horn and J.C. Liang, Z. Phys. **B74**, 197 (1989).

[28] S. Sprunt and J.D. Litster, Phys. Rev. Lett. **59**, 2682 (1987).

[29] S.B. Dierker and R. Pindak, Phys. Rev. Lett. **59**, 1002 (1987).

[30] M. Cheng, J.T. Ho, S.W. Hui, R. Pindak, Phys. Rev. Lett. **59**, 1112 (1987).

[31] M. Paczuski and M. Kardar, Phys. Rev. Lett. **60**, 861 (1988).

[32] D.R. Nelson and R.A. Pelcovits, Phys. Rev. **B16**, 2191 (1977).

[33] R.A. Pelcovits and B.I. Halperin, Phys. Rev. **B19**, 4614 (1979).

[34] S.A. Pikin, Structural Transformations in Liquid Crystals, Gordon and Breach Science Publishers , New York , p. 229 (1991).

[35] A.Z. Patashinskii and V.L. Pokrovskii, 'Fluctuation theory of phase transitions' (Pergamon, Oxford), 1979 p. 139.

[36] E.B. Sirota, P.S. Pershan, L.B. Sorensen and J. Colett, Phys. Rev. **36**, 2890 (1987).

[37] S.Heinekamp, R.Pelcovits, E.Fontes, E. Yi Chen, R.Pindak and R.Meyer, Phys. Rev. Lett., **52**, 1017 (1984);

[38] G. An and M. Schick, Phys. Rev. **B37**, 7534 (1989).

[39] R. Lipowsky, Phys. Rev. Lett. **49**, 1575 (1982).

[40] R. Lipowsky, J. Appl. Phys. **55**, 2485 (1984).

[41] R. Lipowsky, Ferroelectrics **73**, 69 (1987).

[42] B.D. Swanson, H. Stragier, D.J. Tweet and L.B. Sorensen, Phys. Rev. Lett. **62**, 909 (1989).

[43] T. Stoebe, R. Geer, C.C. Huang and J.W. Goodby, Phys. Rev. Lett. **69**, 2090 (1992).

[44] I.Kraus, P.Pieranski, E.Demikhov, H.Stegemeyer, Phys. Rev. E, **48** (1993), 1916.

[45] M.Born and E.Wolf, Principles of Optics, Pergamon Press (1980), chapter 7.6, 327.

[46] D. H. van Winkle and N.A.Clark, Phys. Rev. Lett. **53**, 1157 (1984).

[47] P.E. Cladis, Y. Couder and H.R. Brand, Phys. Rev. Lett. **55**, 2945 (1985).

[48] J. Maclennan, Europhys. Lett. **13**, 435 (1990).

[49] I. Mutabazi, P.L.Finn, J.T. Gleeson, J.W. Goodby, C.D. Andereck and P.E. Cladis, Europhys. Lett. **19**, 391 (1992).

[50] J. Pang, C.D. Muzny and N. Clark, Phys. Rev. Lett. **69**, 278 (1992).

[51] A.E. Jacobs, G. Goldner and D. Mukamel, Phys. Rev. **A45**, 5783 (1992).

[52] J.Maclennan and M.Seul, Phys. Rev. Lett., **69** (1992), 2082.

[53] J.V.Selinger, Z.-G.Wang, R.B.Bruinsma and C.M.Knobler, Phys. Rev. Lett., **70** (1993), 1139.

[54] R. Geer, C.C. Huang, R. Pindak and J.W. Goodby, Phys. Rev. Lett. **63**, 540 (1989).

[55] H. Li, M. Paczuski, M Kardar and K. Huang, Phys. Rev. **B44**, 8274 (1991).

[56] R. Geer, T. Stoebe, C.C. Huang and J.W. Goodby, Phys. Rev. **A46**, 6162 (1992).

[57] S.W. Morris, J.R. de Bruin and A.D. May, Phys. Rev. **B44**, 8146 (1991).

[58] Ch.Bahr and D.Fliegner, Phys. Rev. A, **46**, 7657 (1992).

[59] B.M. Osko, A. Braslau, P.S. Pershan, J. Als-Nielsen and M. Deutsch, Phys. Rev. Lett. **57**, 94 (1986).

[60] K. Myano, Phys. Rev. Lett. **43**, 51 (1979).

[61] D. Beaglehole, A. Braslau, M. Deutsch, P.S. Pershan, A.H. Weiss, J. Als-Nielsen and J. Bohr, Phys. Rev. Lett. **54**, 114 (1985).

[62] J. Als-Nielsen, F. Christensen and P.S. Pershan, Phys. Rev. Lett. **48**, 1107 (1982).

[63] E.B. Sirota, P.S. Pershan, S. Amador and L.B. Sorensen, Phys. Rev. **A35**, 2283 (1987).

[64] S. R. Renn and T. C. Lubensky, Phys. Rev. A **38**, 2132 (1988).

[65] P.Vigman, V.Filev, Sov. Phys. JETP, **42**, 747 (1975).

[66] E.I.Kats, Sov. Phys. JETP, **52**, 327 (1991).

[67] Y.Shnidman and E.Domany, Journ. of Physics C, **14**, L773, (1981).

[68] E.Demikhov, I.Kraus, P.Pieranski, H.Stegemeyer, J.Goodby, A. Slaney and M. Osipov, Ber. Bunsenges. Phys. Chem., **97**, 1376 (1993).

[69] R.R.Netz and S.Hess, Z. Naturforsch., **47a**, 536 (1992).

[70] E. Demikhov, U. Hoffmann and H. Stegemeyer, Journ. de Physique II, to be published.

[71] S.A. Pikin and M.A. Osipov, Ferroelectric Liquid Crystals, (Gordon and Breach, Philadelphia,1991), p. 249.

[72] Ch. Bahr and G. Heppke, Mol. Cryst. Liq. Cryst. **148**, 29 (1987)

[73] E. Demikhov, I. Kraus and P. Pieranski, J. of Physics (Condenced Matter), **6**, Suppl. 23A, 415 (1994).

[74] W.H. Press, B.P. Flannery , S.A. Teukolsky and W.T. Vetterling, Numerical Recipes (Cambridge University Press, Cambridge, 1992) p.645.

[75] K. Binder, Rep. Progr. Phys. **50** (1987) 783.

[76] Ch. Bahr and G. Heppke, Phys. Rev. A **41**, 4335 (1990).

[77] A. Yoshizawa, I. Nishiyama, M. Fukumasa, T. Hirai and M. Yamane, Jap. Journ. of Applied Physics **28**, L1269 (1989).

[78] E. Demikhov, Europhys. Letters **25**, 259 (1994).

[79] E. Demikhov and H. Stegemeyer, to be published in Liquid Crystals.

[80] E. Demikhov, submitted.

[81] S. A. Pikin, A. Strigazzi and A. Sparavigna, in press.

[82] Ch. Bahr and D. Fliegner, Phys. Rev. Lett. **70**, 1842 (1993)

[83] I. Kraus, P. Pieranski and E. Demikhov, to be published.